*Int. J. Electrochem. Sci.*, 10 **(2015)** 7643 - 7659

International Journal of
ELECTROCHEMICAL
SCIENCE
www.electrochemsci.org

# Adsorption of an Azo Dye on Polyaniline/ Niobium Substrate

*Milica Tara-Lunga-Mihali*[1,3], *Nicoleta Plesu*[1,*], *Andrea Kellenberger*[2], *Gheorghe Ilia*[1,3,*]

[1]Institute of Chemistry Timisoara of Romanian Academy, 24 Mihai Viteazul Bvd., 300223-Timisoara, Romania
[2]Politehnica University Timisoara, Faculty of Industrial Chemistry and Environmental Engineering, P-ta Victoriei 2, 300006 Timisoara, Romania,
[3]Vest University Timisoara, Faculty of Chemistry-Biology-Geography, 16 Pestalozzi str., 300115, Timisoara, Romania
[*]E-mail: nplesu@acad-icht.tm.edu.ro

*Received:* 18 May 2015 / *Accepted:* 22 June 2015 / *Published:* 28 July 2015

In this paper the adsorption process of an azo dye on nanostructured polyaniline films electrodeposited on niobium has been investigated using electrochemical impedance spectroscopy. The electrochemical polymerization has been carried such as to obtain PANI films with a highly branched structure and a high specific surface. Based on the impedance results it has been observed that dye concentration affects the adsorption mechanism. The surface adsorption influences the overall mechanism and it could take place simultaneously with the intraparticle diffusion. The relaxation time could estimate the approach of the system to steady state (equilibrium). In diluted dye solution the relaxation time is higher and the intraparticle diffusion could play an important role. Five adsorption isotherms have been used for the mathematical description of adsorption equilibrium data. All the isotherms describe well the adsorption phenomena except Frumkin isotherm. In our case the Langmuir model gave a better fit for concentrated dye solution ($> 3\times10^{-5}$ mol $L^{-1}$) and diffused control Langmuir model for diluted dye solution ($< 2\times10^{-5}$ mol $L^{-1}$). The high correlation coefficient and low standard deviation value gave the best fit for Langmuir isotherm. The change of Gibbs energy has been also evaluated for the adsorption of dye onto polyaniline/niobium substrate. The negative $\Delta G^{\circ}_{ads}$ value (-36.38 kJ $mol^{-1}$) and high value of $K_{ads}$ (33705.67 $mol^{-1}$) obtained in our measurements indicate that adsorption process is spontaneous and a stable adsorbed dye layer on the polyaniline surface is formed. The adsorption takes place via a combination of physical and chemical adsorption but mainly due to physical adsorption.

**Keywords:** adsorption; dye; nanostructured conducting polymers; EIS

## 1. INTRODUCTION

Dye toxic waste in aquatic environments remains nowadays a real problem. Synthetic dyes generally present a complex aromatic molecular structure, are stable and hard to biodegrade [1]. Azo

dyes plays an important role in the textile dyeing process, present a wide range of colours and allowed a quick and better dying. As a consequence, the decolorization or removal of these compounds from the environment remains an important subject.

The treatment of dye-containing effluents uses as main technologies: ion exchange, adsorption, precipitation, biodegradation, membrane filtration, coagulation, flocculation, etc. Photocatalysis is used as a simple and cost effective technique to degrade dyes. As photocatalysts for the degradation of dyes in waste waters, inorganic semiconductors as $TiO_2$ or doped $TiO_2$ are usually used. Adsorption is widely used and it is the most versatile and includes low cost processes for dye removal [2].

Different adsorbents have been used for the removal of dyes like activated charcoal [3], clay [4], agricultural waste or polymers [5, 6]. Nowadays conducting polymers, for instance polyaniline (PANI), are used as adsorbents for the removal of dyes and toxic heavy metals. Conducting polymers gain attention as promising new materials in various technological applications as in sensors [7], rechargeable batteries [8], separation membranes [9] or as corrosion inhibitors [10-12]. PANI remains in the last years in the scientific attention due to its potential applications in micro- and nano-electronics and for sensors, biosensors and biomedical devices construction [13].

Conducting polymers obtained in the form of nanomaterials present interest due to their enhanced properties, different from the properties of corresponding macroscopic form. Nanostructured conducting polymers and their composites are used in synthesis of new intelligent materials designed for use in modern technologies. The nanostructured form of the conducting polymers offers high surface area and improved electrical conductivity [14]. Nanostructured conducting homo- or copolymers of PANI have been obtained by chemical or electrochemical methods. The electrochemical method gives an accurate control of synthesis parameters and it is considered a very convenient way to study the electrochemical properties of PANI nanofibers [15-17].

PANI doped with various organic acids was used as sorbent for the adsorption of methyl orange through chemical interaction. The removal of dyes from aqueous solutions using the chemical interaction of dye molecules with conducting polymer is considered as a green method for removal of organic pollutants from wastewaters. Mahanta et al. [18] have reported the adsorption of anionic (sulphonated) dyes from aqueous solution by doped polyaniline. Also, polyaniline nanotubes base was reported as adsorbent for dye removal from water [19]. The rate of adsorption seems to be enhanced by ultrasonication [20]. PANI in the form of nanotubes can remove anionic (sulfonated) dyes under action of UV and visible light. [20]. Adsorption efficiency of PANI doped with $CuCl_2$ was investigated. Depending on $CuCl_2$ doping levels (0%, 2%, 4%, 6%, 8% and 10%) the highest adsorption efficiency was found for 8% $CuCl_2$ doped PANI [21].

The advantage of electrochemical method in producing conductive polymers i.e. PANI is represented by the accurate control of synthesis parameters and in the same time is a suitable way to study the electrochemical properties of PANI and its interaction with different analytes. Electrochemical impedance spectroscopy (EIS) is a noninvasive method for determining the dielectric properties of an insulating layer present on the surface of a working electrode. By analyzing the data with proper equivalent circuits, the fractional coverage of the adsorbed monolayer can be determined. In order to obtain the isotherm, the values of surface coverage $\theta$ at different dye concentrations ($C_{dye}$) were evaluated from EIS experiments. EIS was chosen as measurement technique for this study

because it is quantitative, non-destructive and able to assess the properties of thin layers over the entire substrate surface.

Information upon interaction between the dye and the PANI surface can be provided by the adsorption isotherm. The adsorption isotherms generally considered include Langmuir, Temkin, Frumkin and Flory-Huggins and El Awady et al. thermodynamic–kinetic model.

This paper reports our attempt to use electrochemical impedance spectroscopy (EIS) to explore the nature of adsorption of azo red dye on the PANI surface. Usually the adsorption studies are realized by UV-VIS spectroscopy. EIS is a suitable method to investigate the interactions of PANI with dye molecules. The method was found to give valuable information regarding adsorption process and allowed to determine critical value of the relaxation times for adsorption (the system approach to equilibrium and the surface saturation), rate constant or degree of adsorption.

To obtain high exposed surface area to improve the adsorbent properties, PANI was electrochemically deposited on electrode (Nb) as we reported. Five isotherms were chosen to fit the EIS experimental data. The highest correlation coefficient gives the best fit for El Awady et al. thermodynamic–kinetic model and Langmuir model, but correlated with the value of standard deviation the Langmuir model was chosen as the best one to describe the adsorption process. The change of Gibbs energy, enthalpy and the $K_{ads}$ evaluated for the adsorption of dye onto PANI/ Nb electrode were found to be -36.38 kJ $mol^{-1}$ and 33705.67 $mol^{-1}$, respectively. These indicate that adsorption process is spontaneous, takes place via a combination of physical and chemical adsorption but mainly due to physical adsorption with the formation of a stable adsorbed dye layer on the PANI surface.

## 2. EXPERIMENTAL

Aniline was freshly distilled under reduced pressure and stored in dark at low temperature. Double distilled water and analytical grade sulphuric acid were used to prepare the electrolyte solutions.

PANI films were obtained by electrochemical polymerization of aniline on niobium substrate from $H_2SO_4$ solution as reported [17]. The potentiodynamic polymerization was performed in an electrochemical cell (standard three-electrode) connected to an Autolab PGSTAT 302N. The working electrode was a Nb disc ( A = 1 $cm^2$), as counter-electrodes two graphite rods were used and as reference electrode a saturated calomel electrode (SCE). EIS measurements were performed in the frequency range from $10^6$ Hz to 1 Hz and AC voltage amplitude of 10 mV, using the FRA Module of Autolab 302N and 60 points with a logarithmic distribution of 10 points per decade were collected for each spectrum. ZView-Scribner Associates Inc. software was used to interpret the experimental electrochemical impedance data with the help of an electrical equivalent circuit by a CNLS Levenberg–Marquardt procedure.

Scanning electron microscopy (SEM) was used for morphology characterization of the PANI films deposited on niobium, using a FEI INSPECT S electron microscope.

*2.1. Adsorption studies*

The adsorption kinetics of azo red dye was investigated using EIS technique. Adsorption of azo red dye was studied under open circuit potential (OCP) condition and the adsorption profile was investigated. The studied dye is a diazo dye derived from 4,4'-diaminobenzanilide and was synthesized and characterized in our laboratory, according to previous study [22]. Figure 1 illustrates the chemical structure of dye. A dye stock solution of $3\times10^{-3}$ mol $L^{-1}$ was prepared by dissolving the dye in distilled water followed by necessary dilutions of this stock solution.

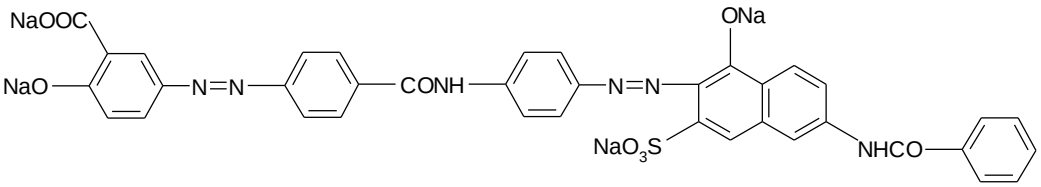


**Figure 1**. Chemical structure of azo red dye.

The values of surface coverage $\theta$, corresponding to different concentrations of dye were used to get best linearity isotherms [23, 24]. The values of surface coverage $\theta$ were obtained from impedance measurements according to equation (1):

$$\Theta = (C_o - C_i) / C_o \qquad (1)$$

where $C_o$ is the capacitance at time $t = 0$ and $C_i$ is the capacitance at any time.

Assumptions of isotherms were made according to the equations (2) – (6) given below:

$$\frac{C}{\theta} = \frac{1}{K_{ads}} + C \qquad (2a) \quad \text{(Langmuir isotherm)}$$

$$R_L = \frac{1}{1 + K_{ads}C} \qquad (2b)$$

$$\theta = \frac{1}{a}\left(\ln C + \ln K\right) \qquad (3) \quad \text{(Temkin isotherm)}$$

$$\ln\left(\frac{\theta}{C(1-\theta)}\right) = \ln K + a\theta \qquad (4) \quad \text{(Frumkin isotherm)}$$

$$\log\left(\frac{\theta}{C}\right) = \log(xK) + x\log(1-\theta) \qquad (5) \quad \text{(Flory–Huggins isotherm)}$$

$$\log(\theta/1-\theta) = \log K^{'} - y\log C \qquad (6) \quad \text{(El Awady et al. thermodynamic–kinetic model)}$$

where $\theta$ is the surface coverage, $C = C_{dye}$ is the dye concentration, $K_{ads}$ is the adsorption equilibrium constant and $a$ is the molecular interaction constant expressing the interaction between adsorbed and adsorbing molecules. In Flory–Huggins isotherm and El Awady et al. thermodynamic–kinetic model, $x$

represents the number of adsorbed water molecules replaced by one molecule of dye and *y* is the number of dye molecules occupying one active site. The equilibrium constant of adsorption from El Awady et al. thermodynamic–kinetic model is $K = K'^{(1/y)}$, where 1/y is the number of the surface active sites occupied by dye molecules.

## 3. RESULTS AND DISCUSSION

### *3.1. PANI electrodeposition on Nb electrode*

For adsorption studies four PANI films were prepared in the same conditions. The deposition of PANI on Nb electrode takes place only after substrate passivation, when Nb is covered by a passivating layer of niobium oxide [17]. After Nb passivation the anodic oxidation of aniline starts at 0.8 V (Fig. 2a) and the electroactive species formed are further capable to initiate then the electropolymerization.

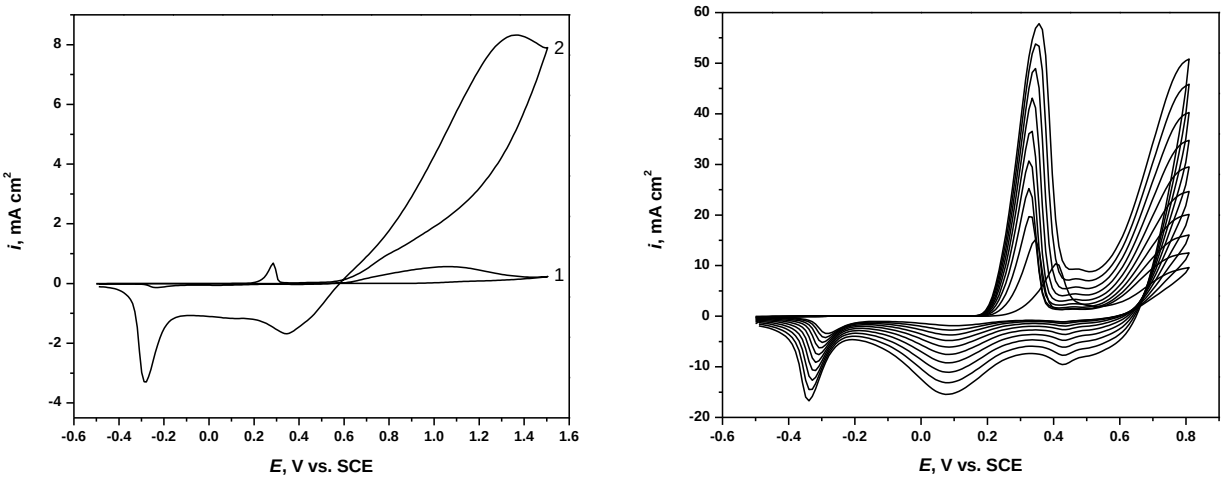


a) b)

**Figure 2.** Electrodeposition of PANI on Nb from 0.4 mol $L^{-1}$ aniline in 1 mol $L^{-1}$ $H_2SO_4$, scan rate 50 mV $s^{-1}$: (a) initiation step and (b) growth step.

After the initiation step the potential window was narrowed to 0.8V to avoid overoxidation of PANI. The propagation step is represented in Fig. 2b and shows an increase of the PANI film thickness as the charge linearly increase with the number of scans. In the CV two pairs of peaks corresponding to the redox transitions of polyaniline from leucoemeraldine to emeraldine and from emeraldine to pernigraniline are observed, together with two pairs of poorly defined redox waves around 0.49 and 0.55 V associated to the redox transitions of degradation products formed during the electropolymerization of aniline [17]. In the CVs an additional reduction peak at -0.34 V was present, attributed to reduction of phenazine units present in the structure of PANI [25]. It has been reported that aniline electropolymerization may also take place via phenazine units [26]. This mechanism can

occur in case of niobium covered with niobium oxide particles, which represent a hydrophobic interface, prone for the adsorption of phenazine nucleates [17].

The deposition charge *Q* was calculated for each PANI film to verify that they have similar masses and thicknesses. Values of 98, 95, 100 and 98 mC have been obtained for the four PANI films, showing a good reproducibility.

The morfology of PANI/Nb shows the presence of PANI network of nanofibers on the surface of oxidized niobium as we expected.

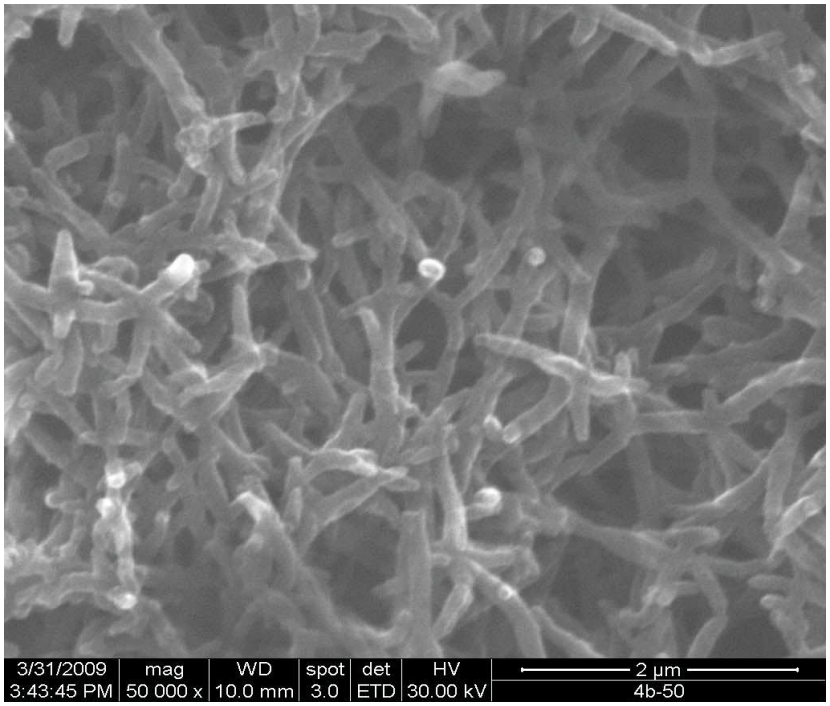


**Figure 3.** SEM image of PANI film on Nb electrode.

The nanostructured morphology of PANI offers high surface area proper for dye retaining. The dye molecules are adsorbed directly on the positively charged PANI sites present on Nb electrode surface via the delocalized π-electrons of the aromatic rings and the negative charges of $COO^-$. Also, the adsorption could take place via hydrogen bond formation between the N–H linkage in PANI and dye. This type of adsorption is more common for protonated *N*-atoms, since the positive charge on the *N*-atoms in PANI chains allows the formation of hydrogen bonds. Unprotonated *N*-atoms may adsorb by direct chemisorption, or by hydrogen bonding to a PANI surface.

### *3.2. EIS of dye retaining process*

Adsorption of azo red dye was studied under OCP condition and the adsorption profile in time was investigated. The impedance plots for PANI electrode in solutions containing different concentrations of azo dye red are shown in Fig. 4.

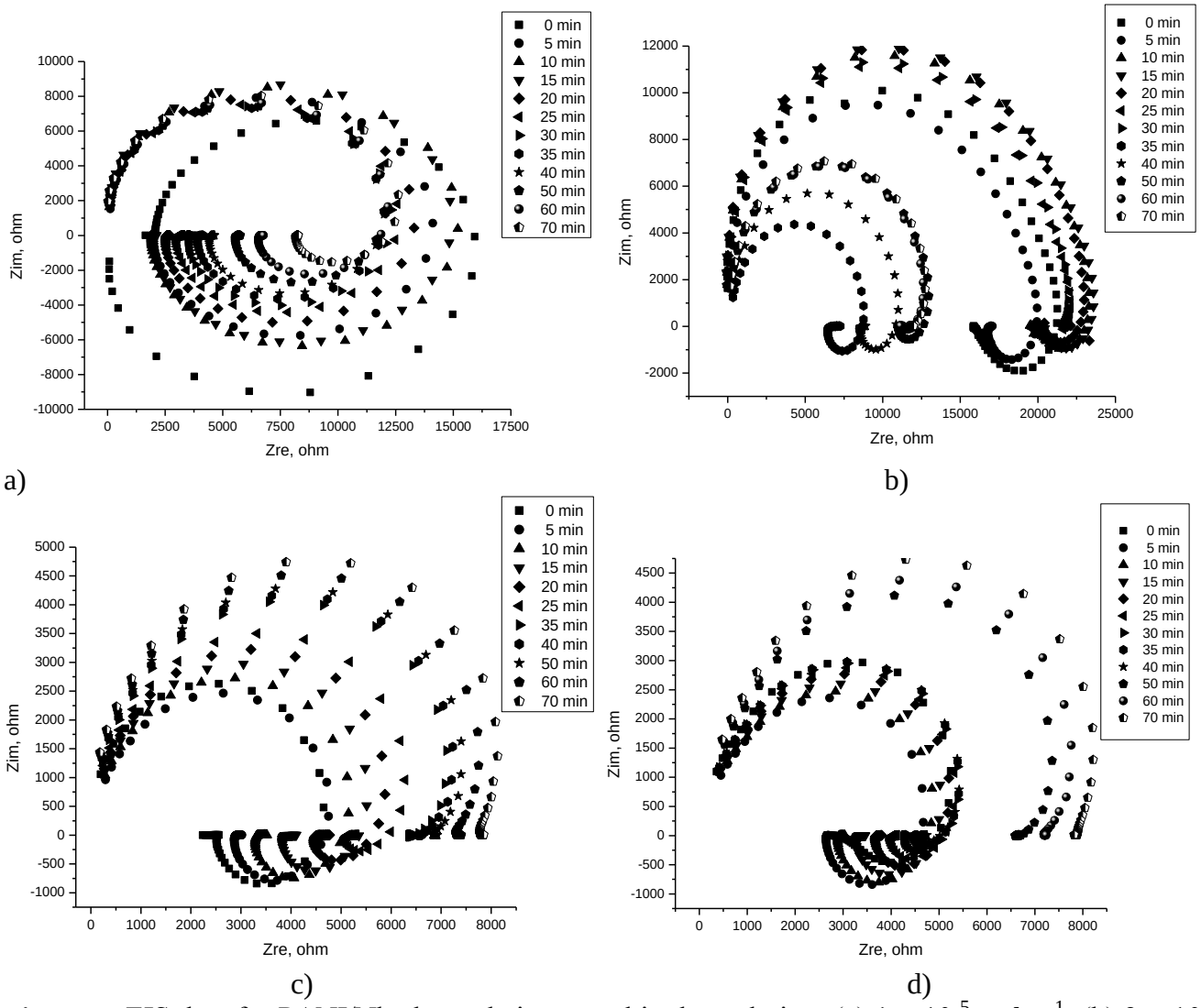


**Figure 4**. EIS data for PANI/Nb electrode immersed in dye solution: (a) $1 \times 10^{-5}$ mol $L^{-1}$; (b) $2 \times 10^{-5}$ mol $L^{-1}$; (c) $3 \times 10^{-5}$ mol $L^{-1}$ and (d) $5 \times 10^{-5}$ mol $L^{-1}$.

In Nyquist plots one semicircle and in Bode plots one time-constant feature are present, which represents the resistive and capacitive properties of the electrode–solution interface. The Nyquist plots contain an inductive loop at low frequencies usually attributed to physical phenomena such as adsorption. With the increase of dye concentration in solution an increase in the diameter of the semicircle and in the maximum of the phase angle was noticed. The impedance parameters are used for evaluation of the interaction between dye and the PANI surface and are obtained by fitting the EIS data with the electric equivalent circuit (EEC) presented in Fig. 5. Similar EEC has been used for modeling interface involving an adsorbed intermediate product [27, 28].

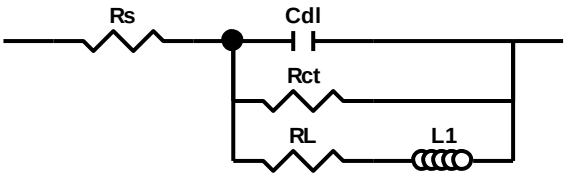


**Figure 5.** The electrochemical equivalent circuit used to fit the impedance measurements.

The EEC includes a resistance - *R*s (the solution resistance between the reference electrode and working electrode) in series with a parallel connection between a capacitor - $C_{dl}$ (double layer capacitance) and a resistance - $R_{ct}$ (the charge transfer resistance). The presence of the low frequency inductive loop was ascribed to the relaxation process of adsorbed species on the PANI electrode surface and was modeled by elements $R_L$ (inductive resistance) and $L$ (inductance) [29, 30]. Fig. 6 displays the evolution of $C_{dl,}$ $R_L$ and $L$ elements determined by fitting the experimental data with the EEC proposed in Fig. 5.

From the EIS data, it was observed that $C_{dl}$ decreases with increase of the time. This phenomenon is generally related to the adsorption of organic molecules on the PANI-metal surface. The adsorption leads to a decrease in the local dielectric constant and/or to an increase in the thickness of the electrical double layer [31**]** as water molecules present at the PANI-electrode interface are replaced through adsorption phenomena by dye molecules from solution and this will result in low capacitance values [32]. Also the larger red azo dye molecules (molar mass 818 g $mol^{-1}$) used in the experiments could increase the double layer thickness and reduce the capacitance [33]. The shape of $C_{dl}$ decrease in Fig. 6a shows a region characterized by a rapid decrease and a plateau region (from ~ 40 min to 270 min) due to complete saturation. After 40 min the adsorption still occurs, but the rate of adsorption is lower. For this reason we considered that dye adsorption reaches saturation at 70 min. $R_L$ is directly proportional to the coverage of dye molecules at the PANI surface (Fig. 6b).

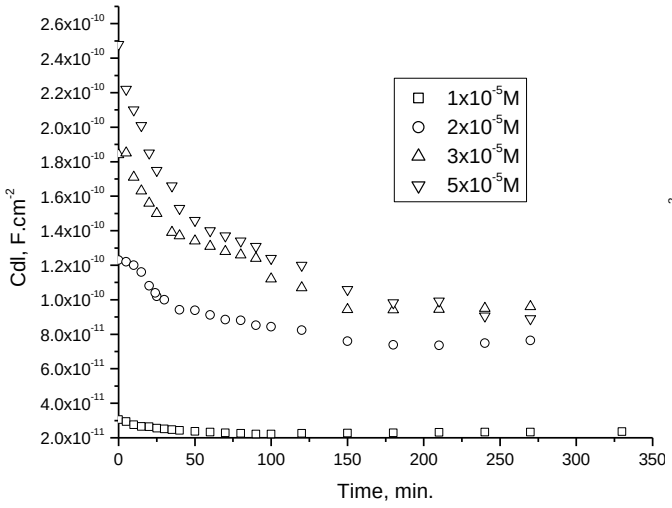


a)

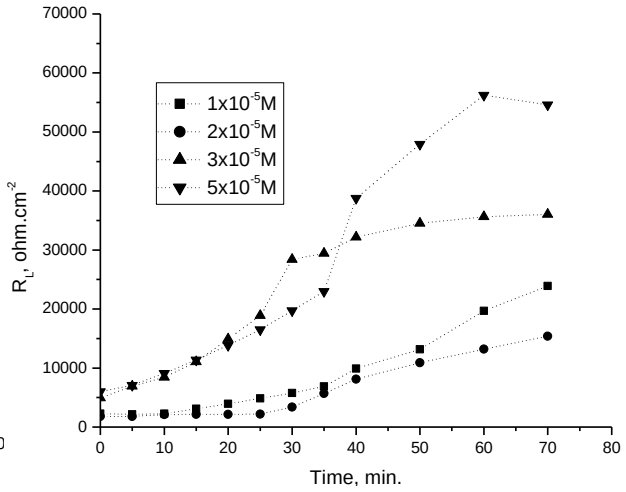


b)

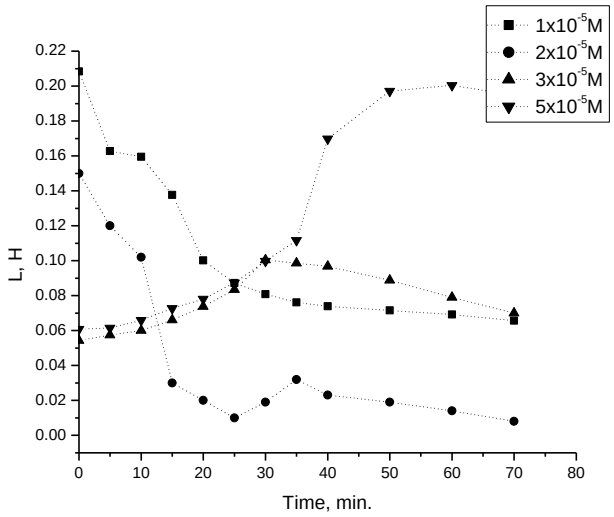


c)

**Figure 6.** Variation of EEC parameters: (a) $C_{dl}$, (b) $R_L$ and (c) $L$ in time for adsorption of azo dye at different concentrations.

The inductor, $L$ arises from adsorption effects and it can be defined as ($L = R\tau$) where $\tau$ is the relaxation time. When adsorption becomes significant, the disappearance of the inductive loop is observed, the value of $L$ decreases as a consequence of the accumulation of dye molecules in the porous PANI layer (Fig. 6c).

The decay of $C_{dl}$ in time shows two regions: a first region of adsorption up to 40 min and another from 40 min to 270 min. In the first minutes of the adsorption, $C_{dl}$ changes rapidly which indicates that dye adsorbs and forms an irreversible layer on the PANI surface. The $C_{dl}$ modification is correlated with the number of contact points between the dye and PANI binding sites. These observations are in agreement with other results reported in the literature [34]. At the beginning of the adsorption (time $t$ = 0) many binding sites are available on PANI surface and many contacts exist between dye and PANI. With the increase of immersion time a layer is produced and the available binging sites decrease. As a result the rate of adsorption decreases. The formation of irreversible layer in the first minutes of immersion and a reversible layer at longer contact times was observed for protein adsorption by Barnabeu [35]. The shape of the capacitance decay is reciprocal of surface coverage and the complete saturation appears at ~40min (see figure 9). The plateau region has been attributed to the saturation of the PANI electrode surface with dye molecules [35]. The rate of adsorption process could be evaluated from the decay of electrode capacitance in the first moments when an irreversible layer of dye is formed on the PANI surface. It is possible to estimate the adsorption rate constant ($k_a$) for initial region, taking into account a molecular reversible adsorption (Langmuir model) and influence of diffusion (Diffusion Controlled Langmuir, DCL model). The Langmuir and DCL models are expressed by equations (7) and (8) respectively.

$$\theta(t) = \left[1 - \exp\left(-k_a t\right)\right] \quad (7)$$

$$\theta(t) = \left[1 - \exp\left(-k_a t^{0.5}\right)\right] \quad (8)$$

The proper model for adsorption kinetics was established representing ln(1-*Θ)* against time or square root of time and taking into account the obtained $R^2$ values for linear regression. The linear regressions of Langmuir and DCL model are presented in Fig. 7 and the adsorption rate constant values are given in Table 1.

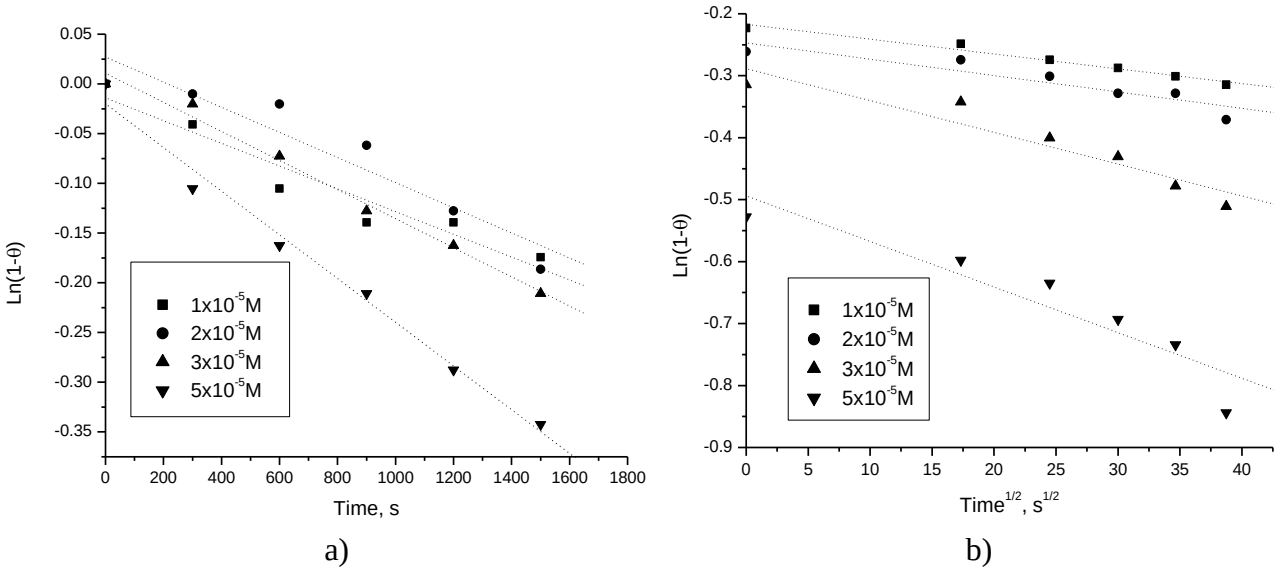


a) b)

**Figure 7.** Adsorption kinetics: (a) Langmuir model showing ln(1- *Θ)* against time and (b) DCL model showing ln(1- *Θ)* against square root of time.

It was observed that both models are suitable for modeling adsorption kinetics. Similar results have been reported for polyaniline nanotubes salt/silica composite tested as adsorbent for anionic dye from water [36], where intraparticle diffusion seems to be also involved in the adsorption process but it is not the only rate-limiting mechanism and surface adsorption and intraparticle diffusion were probable to take place at the same time.

**Table 1.** Adsorption rate constant values obtained using Langmuir and DCL model

| Dye concentration, mol $L^{-1}$ | Langmuir model | | DCL model | |
|---|---|---|---|---|
| | $k_a$ [$s^{-1}$] | $R^2$ | $k_a$ [$s^{-1/2}$] | $R^2$ |
| $1 \times 10^{-5}$ | $12.72 \times 10^{-3}$ | 0.965 | $2.39 \times 10^{-3}$ | 0.986 |
| $2 \times 10^{-5}$ | $10.26 \times 10^{-3}$ | 0.950 | $2.64 \times 10^{-3}$ | 0.921 |
| $3 \times 10^{-5}$ | $13.73 \times 10^{-3}$ | 0.995 | $5.13 \times 10^{-3}$ | 0.981 |
| $5 \times 10^{-5}$ | $23.88 \times 10^{-3}$ | 0.994 | $7.36 \times 10^{-3}$ | 0.931 |

Based on the results it was observed that dye concentration affects the adsorption mechanism. This indicates that besides the surface adsorption, the intraparticle diffusion plays an important role and could take place simultaneously. In our case for concentrated dye solution higher than $3 \times 10^{-5}$ mol

$L^{-1}$ the Langmuir model gave a better fit and for diluted dye solution lower than $2 \times 10^{-5}$ mol $L^{-1}$ the DCL model. This could be supported also by the evolution of $L$ in time (Fig. 6c) where two situations were observed depending on dye concentration. For diluted dye solution a decrease of $L$ in time is observed as a consequence of the accumulation of dye molecules in the porous PANI layer. For concentrated dye solution an increase of $L$ in time was observed due to an autocatalytic mechanism of adsorption, which means that an increase of surface coverage stimulates the further adsorption [37]. The increase of $R_L$ value in time for all dye concentration was observed (Fig. 6b). This increase could be correlated with the increase of surface coverage at high dye concentration.

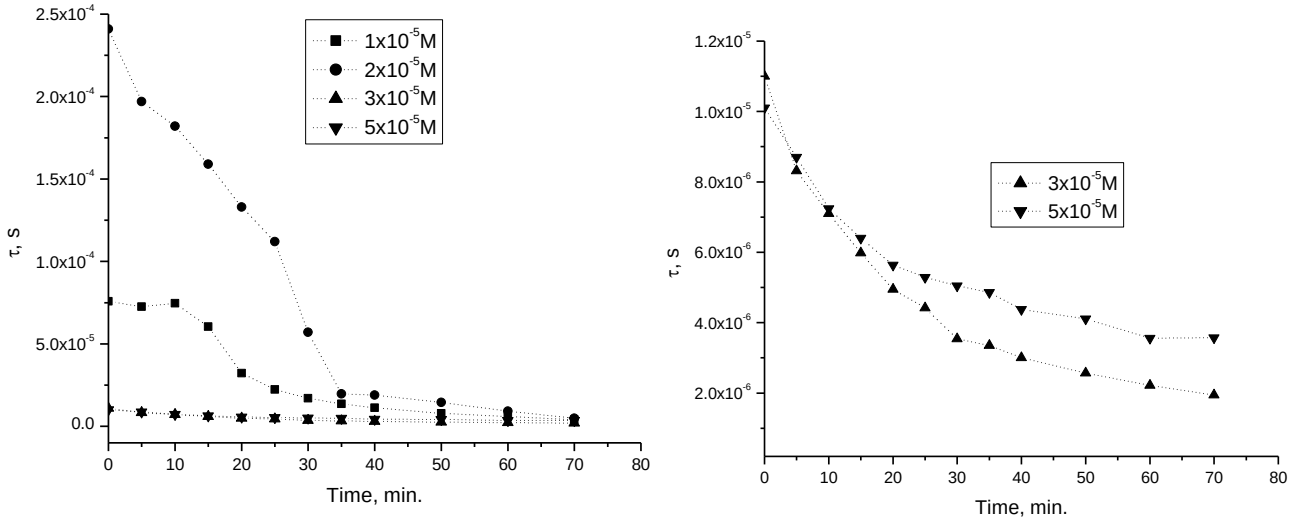


a) b)

**Figure 8.** The variations of the relaxation with a) dye concentrations in time b) details for concentrated solutions.

Taking into account that $\tau$ is the relaxation time for adsorption of dye on PANI surface, the variations of the relaxation time, $\tau = L/R_L$, with dye concentrations in time could give an explanation of the influence of dye concentration. The relaxation time is a measure of the rate correlated with the system approach to steady state (equilibrium). Since the relaxation time in diluted dye solution is higher it means that dye molecules need longer time to reach the PANI surface which leads to an increase in the time required by the system to return back to its equilibrium state and for this situation the intraparticle diffusion could play an important role (Fig. 8a).

The relaxation time decreases with increasing dye concentration due to autocatalytic adsorption mechanism and as a consequence the time needed to attain the equilibrium decreases (Fig. 8b). Moreover, it is observed that the relaxation times concentrate to a critical value at 35 min after which the $\tau$ values remain almost constant for all concentrations. The critical time indicates an approach to equilibrium and the surface saturation.

Based on the capacitance values using equation 1, the degree of surface coverage ($\theta$) of the electrode during the adsorption was calculated. Fig. 9 illustrates the variation in time of surface coverage for all dye solution concentrations.

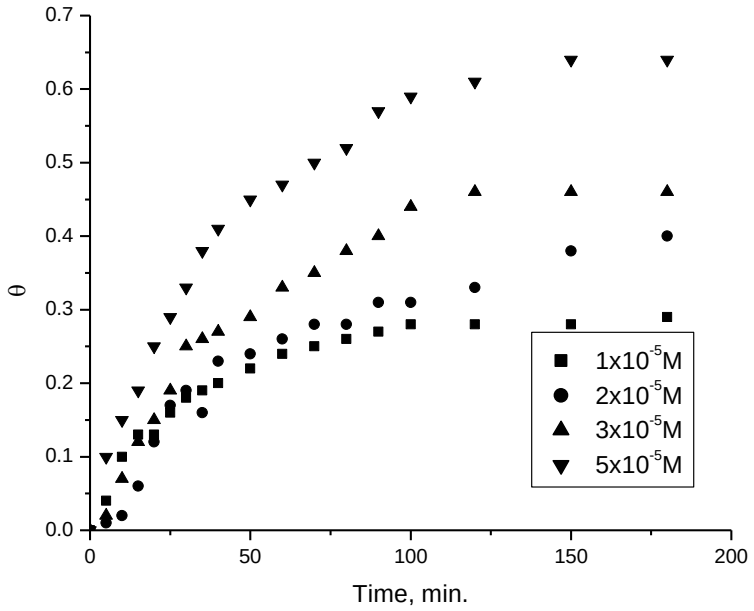


**Figure 9.** The electrode surface coverage variation in time for all dye solution concentrations.

Basic information on the interaction between the azo red dye molecules and the PANI/Nb surface can be suggested by the adsorption isotherms. Attempts were made to fit the $\theta$ values to various isotherms including Langmuir, Temkin, Frumkin, Flory-Huggins and El Awady et al. thermodynamic–kinetic model. The correlation coefficient ($R^2$) and low standard deviation (SD) were used to choose the proper isotherm capable to fit experimental data (Table 2). Fig. 10 shows the linear plots for all considered isotherms obtained using equations (2) – (6).

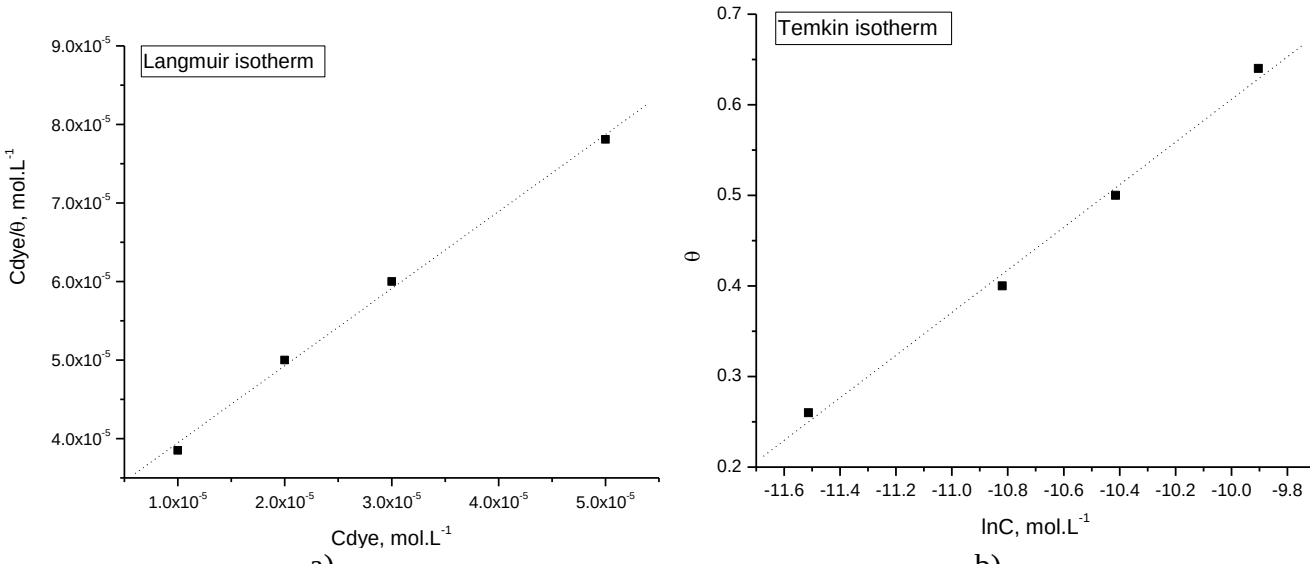

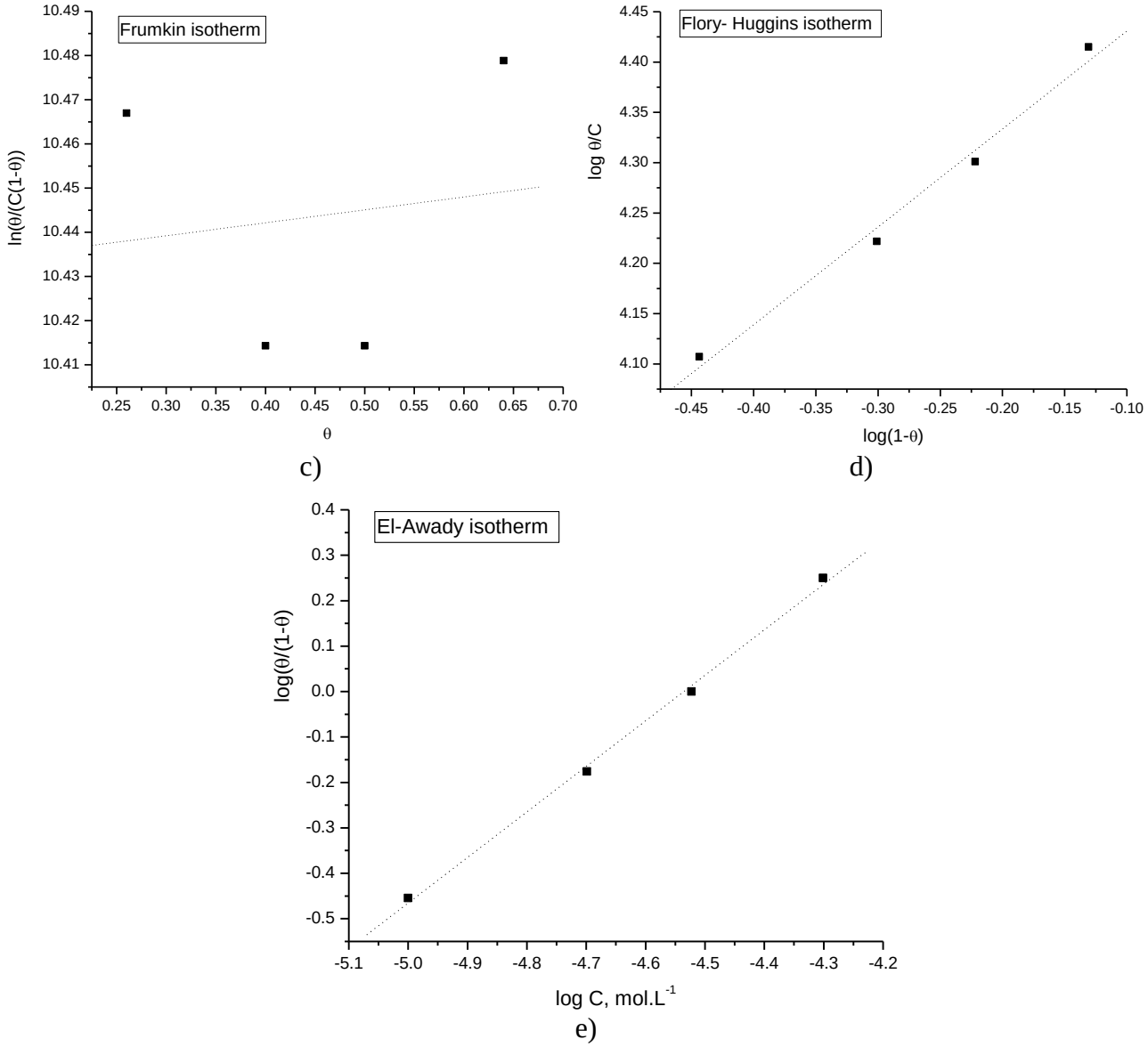


**Figure 10**. (a) Langmuir, (b) Temkin, (c) Frumkin, (d) Flory–Huggins isotherms and (e) El Awady et al. thermodynamic–kinetic model.

The values of $K_{ads}$, $R_{Langmuir}$, a, x, K', 1/y and $\Delta G^{\circ}_{ads}$ calculated by all adsorption isotherms are given in Table 2.

The values obtained for slopes in the Langmuir model were less than unity and indicate the existence of interactions between the adsorbed dye molecules and PANI surface. The validity of Frumkin isotherm is restricted by correlation coefficient and suggests that one adsorption could involve more or less than one dye molecule per active site. Therefore, Flory-Huggins isotherm and El Awady et al. thermodynamic–kinetic model were also used to explain the existence of interactions. Values of the size parameter *x* in Flory-Huggins isotherm greater than one imply the formation of multilayers of dye on the PANI surface and a value of *x* less than one, means that a dye molecule will occupy more than one active site.

**Table 2.** The values of $K_{ads}$, $R_{Langmuir}$, a, x, K', 1/y and $\Delta G^{\circ}_{ads}$ calculated by all adsorption isotherms

| Model | Parameters | $R^2$ | SD |
|---|---|---|---|
| Langmuir | $K_{ads}$ = 33705.67 $mol^{-1}$ | 0.998 | $1.15 \times 10^{-6}$ |
| | $R_{Langmuir}$ = 0.70 ($C_{dye} = 1 \times 10^{-5}$ mol $L^{-1}$)<br>0.54 ($C_{dye} = 2 \times 10^{-5}$ mol $L^{-1}$)<br>0.44 ($C_{dye} = 3 \times 10^{-5}$ mol $L^{-1}$)<br>0.32 ($C_{dye} = 5 \times 10^{-5}$ mol $L^{-1}$) | | |
| | $\Delta G^{\circ}_{ads}$ = - 36.381 kJ $mol^{-1}$ | | |
| Temkin | $K_{ads}$ = 287.793 $mol^{-1}$ | 0.997 | $1.53 \times 10^{-2}$ |
| | a = 4.26 | | |
| | $\Delta G^{\circ}_{ads}$ = - 24.382 kJ $mol^{-1}$ | | |
| Frumkin | $K_{ads}$ = 33875.25 $mol^{-1}$ | 0.137 | $4.15 \times 10^{-2}$ |
| | a = 0.02927 | | |
| | $\Delta G^{\circ}_{ads}$ = - 36.394 kJ $mol^{-1}$ | | |
| Flory-Huggins | $K_{ads}$ = 34690.98 $mol^{-1}$ | 0.994 | $1.76 \times 10^{-2}$ |
| | x = 0.972 | | |
| | $\Delta G^{\circ}_{ads}$ = -36. 454 kJ $mol^{-1}$ | | |
| El-Awady | K' = 35460.10 $mol^{-1}$<br>$K_{ads}$ = 34348.32 $mol^{-1}$ | 0.999 | $1.81 \times 10^{-2}$ |
| | y = 1.003 | | |
| | $\Delta G^{\circ}_{ads}$ = - 36.406 kJ $mol^{-1}$ | | |

The number of active sites of the surface occupied by one molecule of dye is given by the value of 1/*y* from El-Awady model, which gives indication about the possibility of multilayer formation. If ratio is less than unity the formation of multilayers of adsorbed molecules on the surface is possible, while the value of 1/*y* greater than unity means that adsorbed molecule plausible occupy more than one active site [39].

The straight line relationship was obtained for Langmuir, Temkin, Flory-Huggins and El-Awady isotherms with a correlation coefficient over 0.99. The highest value was obtained for El-Awady isotherm (0.999).

The Langmuir adsorption isotherm ($R^2$ = 0.998) was found to be suitable for the experimental findings closed to the El-Awady model ($R^2$ = 0.999). The highest correlation coefficient gives the best fit for El Awady et al. thermodynamic–kinetic model, but it should be correlated with the value of standard deviation. SD value is an indication of the deviation of the experimental data points from expected value. A low SD value shows that data meet the assumptions of the model, while a high SD value implies that the data points are expanded over a wider range of values. In our case both lower SD value and high correlation factor was obtained for Langmuir model. Also, the values of *x* and 1/*y* (Table 2) in our study are closed to unity pointing out rather to an adsorption with the formation of a monolayer of adsorbed molecules on the surface (resembling Langmuir model). These observations indicate that Langmuir model describes most accurately the adsorption process for selected red azo dye on PANI nanofibers.

Based on the $K_{ads}$ determined for Langmuir isotherm the dimensionless separation factor, $R_{Langmuir}$ [38], described by eq. (2b) was calculated. $R_{Langmuir}$ indicates in the case of a smaller value a high favorable adsorption process, an unfavorable adsorption in the case of $R_{Langmuir} > 1$, linear adsorption for $R_{Langmuir} = 1$ and favorable for $0 < R_{Langmuir} < 1$. If $R_{Langmuir} = 0$ the adsorption process is irreversible. The calculated values of $R_{Langmuir}$ for different dye concentrations (Table 2) are less than unity, confirming that the adsorption processes on PANI are favorable for all concentrations.

Based on the value obtained for $K_{ads}$ the free energy of adsorption ($\Delta G^{o}_{ads}$), was calculated using eq. (9):

$$\Delta G^{\circ}_{ads} = -RTLn(55.5K_{ads}) \quad (9)$$

where R is the universal gas constant (8.314 J $mol^{-1}$ $K^{-1}$) and T is the absolute temperature in Kelvin, $K_{ads}$ is the adsorption equilibrium constant, $\Delta G^{o}_{ads}$ is the standard free energy of adsorption, 55.5 is the concentration of water in the solution in mol $dm^{-3}$.

If the value of $\Delta G^{\circ}_{ads}$ is lower than -20 kJ $mol^{-1}$ the adsorption consists of electrostatic interactions between charged molecules and a charged surface which indicates a physical adsorption. If the value is higher than -40 kJ $mol^{-1}$ chemisorption takes place due to charge sharing or transfer from the molecules to the surface as a coordinate type of bond [40]. $K_{ads}$ represents the strength between adsorbate and adsorbent. Larger values of $K_{ads}$ imply more efficient adsorption.

The values of $\Delta G^{o}_{ads}$ and $K_{ads}$ obtained from Langmuir isotherm ($\Delta G^{o}_{ads}$ ~ - 36.38 kJ $mol^{-1}$ and $K_{ads}$ ~33.7 $kmol^{-1}$) are comparable with those obtained from El Awady et al. thermodynamic–kinetic model and Flory-Huggins isotherm (Table 2). The adsorption is spontaneous process and takes place via a combination of physical and chemical adsorption but mainly due to physical adsorption. The adsorption of azo red dye on PANI/Nb has a lower $\Delta G^{o}_{ads}$ value than the value of $\Delta G^{o}_{ads}$ of -12.61 kJ $mol^{-1}$ reported for the adsorption process of tartrazine onto PANI/$Fe_2O_3$ [41].

## 4. CONCLUSIONS

PANI films electrochemically deposited on Nb electrode present a highly branched structure and a high specific surface with dye retaining capacity. The EIS results indicate that surface adsorption and intraparticle diffusion mechanism play an important role and they could take place simultaneously. The Langmuir model gave a better fit for concentrations higher than $3 \times 10^{-5}$ mol $L^{-1}$ and Diffused Control Langmuir model for concentrations lower than $2 \times 10^{-5}$ mol $L^{-1}$. The relaxation time indicates that the system approaches to steady state (equilibrium). In diluted dye solution the relaxation time is higher and the intraparticle diffusion could play an important role. The isotherms describe well the adsorption phenomena except Frumkin isotherm. The high correlation coefficient and low SD value give the best fit for Langmuir isotherm. This model describes most accurately the adsorption process for red azo dye on the surface of PANI nanofibers. The change of Gibbs energy has been also evaluated for the adsorption of dye onto PANI/ Nb electrode. The negative $\Delta G^{\circ}_{ads}$ value and high value of $K_{ads}$ suggest that adsorption process is spontaneous with the formation of a stable adsorbed dye

layer on the PANI surface. The adsorption takes place via a combination of physical and chemical adsorption.

## References


1. M. El Haddad, R. Mamouni, R. Slimani, N. Saffaj, M. Ridaoui, S. El Antri and S. Lazar, *J. Mater. Environ. Sci.*, 3 (2012) 1019
2. A. M. Salem, A. F. Al-Ghonemiy and A. B. Zaki., *Appl. Catal. B-Environ.*, 91 (2009) 59
3. Y.C. Sharma, S.N. Uma and G.F. Upadhyay, *J. Appl. Sci. Environ. Sanit.*, 4 (2009) 21
4. K.R. Ramkrishna and T. Viaraghavan, *Water Sci. Technol.*, 36 (1997) 189
5. C. Namasivayam, D. Prabha and M. Kumutha, *Bioresource Technol.*, 64 (1998) 77
6. G. McKay, G. Ramprasad and P.P. Mowli, *Water, Air and Soil Poll.*, 29 (1986) 273
7. N.B. Clark and L.J. Maher, *React. Funct. Polym.*, 69 (2009) 594
8. M. Tara-Lunga-Mihali, N. Plesu, L. Macarie, S. Iliescu and G. Ilia, *Pure Appl. Chem*., 86 (2014) 1853
9. D.C. Bhattacharya, J.M. Mukherjee, Y. Gohil, S. Kumar and S. Kundu, *Desalination*, 225 (2008) 366
10. B. Wessling and J. Posdorfer, *Electrochim. Acta*, 44 (1999) 2139
11. W.-K. Lu, L. Elsenbaumer and B. Wessling, *Synth. Met*., 71 **(**1995) 2163
12. N. Pleşu, G. Ilia, A. Pascariu and G. Vlase, *Synth. Met.*, 156 (2006) 230
13. J. Unsworth, B.A. Lunn, P.C. Innis, Z. Jin, A. Kaynak and N.G. Booth, *J. Intel. Mat. Syst. Str.*, 3 (1992) 380
14. V. Golob, A. Vinder and M. Simonic, *Dyes Pigm*., 67 (2005) 93
15. H.H. Zhou, S.Q. Jiao, J.H. Chen, W.Z. Wei and Y.F. Kuang, *Thin Solid Films*, 450 (2004) 233
16. H. Zhou, J. Wen, X. Ning, C. Fu, J. Chen and Y. Kuang, *Synth. Met*., 157 (2007) 98
17. A. Kellenberger, N. Plesu, M. Tara-Lunga Mihali and N. Vaszilcsin, *Polymer*, *54* (2013) 3166
18. D. Mahanta, M. Giridhar, S. Radhakrishnan and P. Satish, *J. Phys. Chem. B*, 113 (2009) 2293
19. M.M. Ayad and A. Abu El-Nasr, *J. Phys. Chem. C*, 114 (2010) 14377
20. V.N. Nerkar, R.S. Kargirwar, S.B. Kondawar, D.V. Burghate and P.D. Burghate, *Int. J. Sci. Res.*, 4 (2013) 195
21. D. Bingola, S. Veli, S. Zora and U. Ozdemirb, *Synth. Met*., 162 (2012) 1566
22. G.M. Simu, S.L. Funar-Timofei, S.G. Hora, W.E. Schmidt, L. Kurunczi, E.N.V. Sisu and N. Morin, *Rev.Chim-Bucharest*, 53 (2002), 826
23. S. John, K. M. Ali and A. Joseph, *Bull. Mater. Sci*., 34 (2011) 1245
24. M. Bouklah, B. Hammouti, M. Lagrene and F. Bentiss, *Corros. Sci.*, 48 (2006) 2831
25. Z. Puskás and G. Inzelt, *J. Solid State Electrochem*., 8 (2004) 828
26. J. Stejskal, I. Sapurina and M. Trchova, *Prog. Polym. Sci*., 35 (2010) 1420
27. G. Zhang, C. Chen, M. Lu, C. Chai and Y. Wu, *Mater. Chem. Phys*., 105 (2007) 331
28. F. Farelas, M. Galicia, B. Brown S. Nesic and H. Castaneda, *Corros. Sci.*, 52 (2010) 509
29. M. Lebrini, F. Robert, P.A. Blandinières and C. Roos, *Int. J. Electrochem. Sci.*, 6 (2011) 2443
30. M.A. Amin, S.S. Abd El-Rehim, E.E.F. El-Sherbini and R.S. Bayyomi, *Electrochim. Acta*, 52 (2007) 3588
31. E. McCafferty and N. Hackerman, *J. Electrochem. Soc*., 119 (1972) 146
32. P. Li, J. Y. Lin, K. L. Tan and J. Y. Lee, *Electrochim. Acta*, 42 (1997) 605
33. S. S. Abdel Rehim, O. A. Hazzazi, M. A. Amin and K. F. Khaled, *Corros. Sci*., 50 (2008) 2258
34. E.S. Moulton, N.J. Barisci, A. Bath, R. Stella and G.G. Wallace, *Langmuir*, 21 (2005) 316
35. P. Barnabeu, L. Tamisier, A. De Cesare and A. Carpani, *Electrochim. Acta*, 33 (1988) 1129
36. M.M Ayad and A. Abu El-Nasr, *J. Nanostruct. Chem.*, 3 (2012) Art. No. 3
37. A. Sadkowski, *Electrochim. Acta*, 49 (2004) 2259

38. L.D Mall, V.C. Srivastava, N.K. Agrawal and Mishra, *Colloids Surf. A*, 264 (2005) 17
39. A.K. Singh and M.A. Quraishi, *Corros. Sci., 53* (2011) 1288
40. M.K. Gomma and M.H. Wahdan, *Mater. Chem. Phys.*, 39 (1995) 209
41. S.A. Jebreil, *International Journal of Chemical, Nuclear, Materials and Metallurgical Engineering*, 8 (2014)1356